Journal of Volcanology and Geothermal Research 455 (2024) 108200

Contents lists available at ScienceDirect

Journal of Volcanology and Geothermal Research

journal homepage: www.journals.elsevier.com/journal-of-volcanology-and-geothermal-research

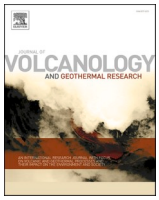

Volcanomagnetic signals related to the 2021 Tajogaite volcanic eruption in the Cumbre Vieja rift (La Palma, Canary Islands)

Isabel Blanco-Montenegro [a,e,*], José Arnoso [b,e], Nieves Sánchez [c], Fuensanta G. Montesinos [d,e], David Gómez-Ortiz [f,g], Iacopo Nicolosi [h], Emilio Vélez [b,e], Maite Benavent [d,e]

[a] Departamento de Física, Escuela Politécnica Superior, Universidad de Burgos, Avda. de Cantabria s/n, 09006 Burgos, Spain
[b] Instituto de Geociencias (IGEO), CSIC-UCM, C/Doctor Severo Ochoa, 7, 28040 Madrid, Spain
[c] Instituto Geológico y Minero de España (IGME, CSIC), Unidad Territorial de Canarias, C/Alonso Alvarado, 43, 2A, 35003 Las Palmas de Gran Canaria, Spain
[d] Facultad de Ciencias Matemáticas, Universidad Complutense de Madrid, Plaza de Ciencias, 3, 28040 Madrid, Spain
[e] Research Group 'Geodesia', Universidad Complutense de Madrid, Spain
[f] Departamento de Biología y Geología, Física y Química Inorgánica, ESCET, Universidad Rey Juan Carlos, C/Tulipán s/n, Móstoles, 28933 Madrid, Spain
[g] Research Group 'Geofísica y geoquímica Ambiental', Universidad Rey Juan Carlos, Spain
[h] Istituto Nazionale di Geofisica e Vulcanologia, Via di Vigna Murata 605, 00143 Roma, Italy

ARTICLE INFO

Keywords:
Volcanomagnetism
Geomagnetism
Volcanic islands
La Palma
Tajogaite
Canary Islands

ABSTRACT

After almost 50 years of quiescence, the Cumbre Vieja rift in La Palma underwent a reactivation process that culminated in the eruption of the Tajogaite volcano from September 19 to December 13, 2021. In July 2021, a magnetic station (CFU) was deployed in the western flank of the Cumbre Vieja rift, 2 km away from the site where the eruptive vents would open two months later. In September 2021, a second magnetic station (SAN) was installed near the southern end of the rift. In this paper we study two months of geomagnetic data at CFU before the eruption and three months of geomagnetic data at SAN during the eruption. The analysis of these time series revealed a magnetic signal at the CFU station with an amplitude of 10 nT and a duration of 10 days by mid-August, one month before the eruption onset. We studied possible correlations with other physical parameters (ground deformation, long-period and very-long-period seismic activity) and concluded that this signal could be related to changes in the magnetization of rocks beneath the volcanic edifice caused by magma intrusion and volcanic/hydrothermal fluids circulation preceding the eruption. At the SAN magnetic station, the time series suggests that a slight decrease in the geomagnetic field could reflect the end of the eruptive process.

1. Introduction

Fifty years after the last eruption on the island of La Palma (Canary Islands, see location in Fig. 1a), the Cumbre Vieja rift experienced a reactivation that culminated in an eruption in September 2021. This eruption lasted three months and destroyed thousands of buildings, banana plantations and civil infrastructures, causing a huge impact on the lives of the island's inhabitants. Although early signs of reawakening were detected in 2017–2018, with the occurrence of two seismic swarms at depths of more than 20 km (Torres-González et al., 2020; Fernández et al., 2021), precursory signals on the months preceding the eruption onset (September 19th) were scarce. The eruptive process triggered in just eight days, which was the time lapse required for the magma to reach the surface from a reservoir located at the base of the crust, accompanied by intense volcanotectonic seismic activity that started on September 11th. This behavior demonstrates that the identification of any possible precursor parameter, capable of informing about the changes that are taking place within the volcanic system months before an eruption onset, is extremely important.

The continuous recording of the geomagnetic field at a certain site over the Earth's surface contains a variety of signals of different amplitude and frequency with sources both inside and outside the Earth. The most important contribution is the main field, with amplitudes of several tens of thousands nT, originated in the Earth' outer core, which varies slowly in time (secular variation). The local or crustal field, with intensity from several hundreds to a few thousands nT in volcanic areas, is due to the presence of magnetic minerals contained in rocks and it also represents an important part of the total magnetic field. This field is

* Corresponding author at: Departamento de Física, Escuela Politécnica Superior, Universidad de Burgos, Avda. de Cantabria s/n, 09006 Burgos, Spain.
E-mail address: iblanco@ubu.es (I. Blanco-Montenegro).

https://doi.org/10.1016/j.jvolgeores.2024.108200
Received 30 May 2024; Received in revised form 20 September 2024; Accepted 28 September 2024
Available online 2 October 2024

mostly static, which means that it is constant in time unless dynamic changes beneath the surface occur, capable of changing the magnetism of rocks. The most variable and unpredictable component of the magnetic field is the external field, with sources in the ionosphere and magnetosphere and periods from seconds to days, which induces secondary time-varying magnetic fields at a local scale due to interaction with the crustal electrical conductivity structure (Parkinson, 1983).

In addition, in geological environments where changes in the crust can occur in time scales of the order of days to months or even years, a fourth magnetic field can be summed up to the previous constituent fields. This is the case of active volcanoes, where volcanic activity can modify the magnetic properties of crustal rocks and produce a "volcanomagnetic" field which varies in time. Thus, changes in the thermal and stress state of the crust related with volcanic fluid migration, magma upwelling, dyke intrusion, etc. can alter the rocks' magnetizations and produce small-amplitude, transient magnetic fields which will be superimposed to the sum of constituent geomagnetic fields mentioned before. After the pioneering works carried out several decades ago in Mt. Ruapehu (New Zealand) (Johnston and Stacey, 1969), Kilauea (Hawaii) (Davis et al., 1973) and La Soufrière (Guadeloupe) (Pozzi et al., 1979), magnetic studies in different volcanoes around the world have revealed that volcanomagnetic signals sometimes accompany volcanic processes

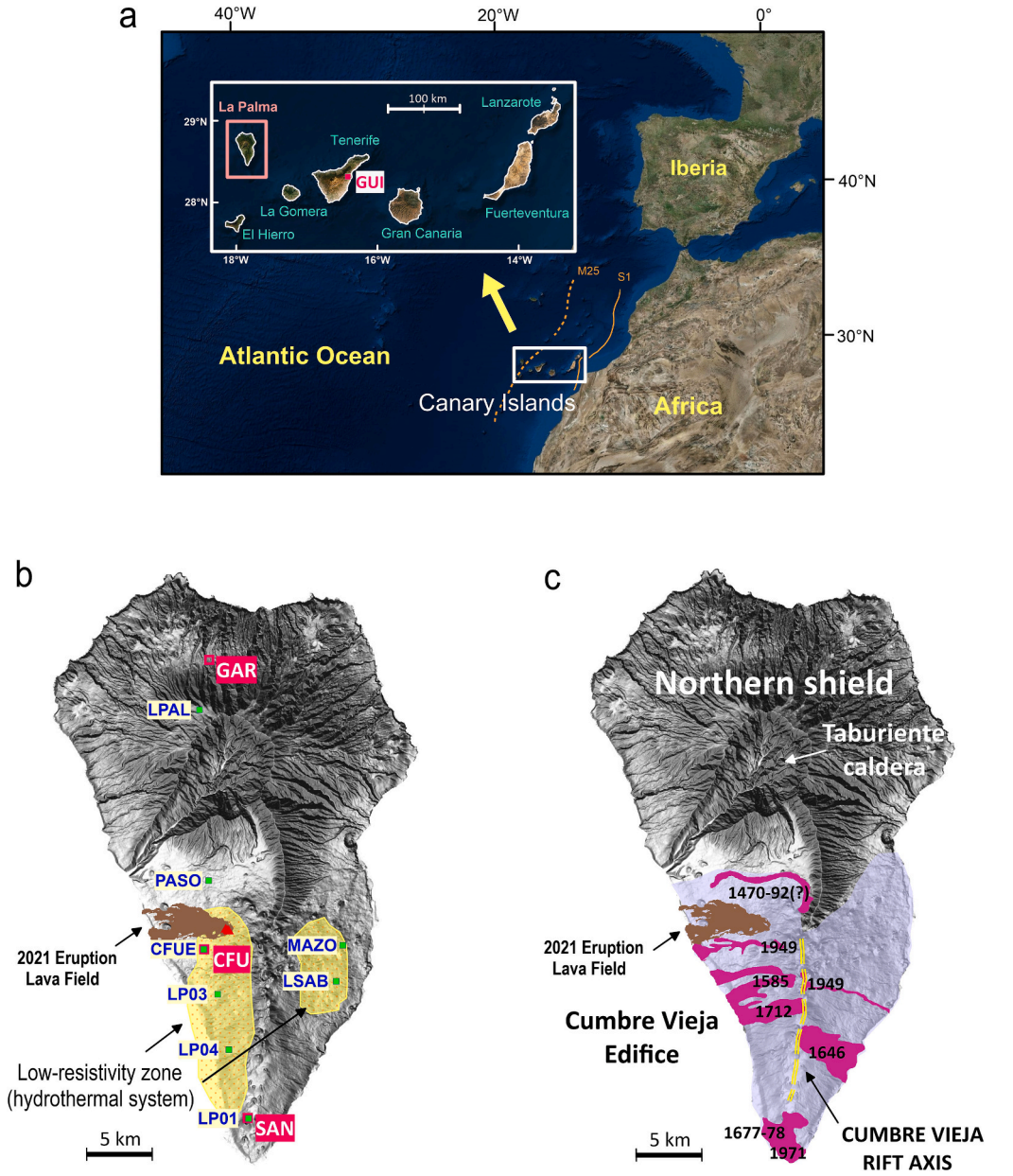

Fig. 1. a) Geographical location of the Canary Islands in the Atlantic Ocean, bounded by marine magnetic anomalies M25 and S1 (Verhoef et al., 1991), with La Palma Island in the western part of the archipelago (inset). The location of the Güímar geomagnetic observatory, GUI, (National Geographic Institute of Spain, IGN) in Tenerife is shown. b) Shaded relief of La Palma and location of CFU, SAN and GAR magnetic stations. The blue labels identify the GNSS stations used for deformation monitoring (CFUE, LSAB, and PASO owned by the Institute of Geosciences of Spain, CSIC-UCM; LP01, LP03, LP04, and LPAL owned by the IGN of Spain; MAZO owned by GRAFCAN). The yellow areas show the boundaries at a depth of ~3 km b.s.l. of the low-resistivity bodies detected by magnetotelluric sounding (Di Paolo et al., 2020). The eruptive vents (red triangles) and lava field (brown area) of the 2021 eruption are also displayed. c) Simplified geological sketch of La Palma, showing the Northern Shield and the Cumbre Vieja edifice, where the lava fields of the historical eruptions are displayed in purple, indicating the year of the eruption. The Cumbre Vieja rift axis is marked in yellow. (For interpretation of the references to colour in this figure legend, the reader is referred to the web version of this article.)

(Davis et al., 1984; Zlotnicki and Le Mouel, 1988; Sasai et al., 1990; Zlotnicki et al., 1993; Tanaka, 1993; Del Negro and Ferrucci, 1998; Hurst et al., 2004).

Some well-studied volcanoes, such as Piton de la Fournaise (Réunion) (Zlotnicki and Le Mouel, 1988; Zlotnicki et al., 1993) and Etna (Sicily) (Del Negro et al., 2004; Napoli et al., 2008), have been monitored for years with the continuous recording of the magnetic field acquired by an array of magnetometers deployed in different parts of the volcano that allowed to study the volcanomagnetic field both in space and time. However, magnetic monitoring does not often take part of the usual volcano surveillance techniques, which are typically based on seismic activity and ground deformation. This is possibly due to difficulties related with the maintenance of an array of magnetometers around a volcano for years and to the small amplitudes of the expected volcanomagnetic signals, which make their isolation from the measured geomagnetic field a challenging task.

In this work, we present the results of the analysis of the geomagnetic field time series acquired before and during the 2021 eruption at two sites in the area affected by the volcanic reactivation (Fig. 1). A first magnetometer was deployed on July 22, 2021, to record the magnetic field in the western flank of Cumbre Vieja, 2 km away from the location where the eruptive vents would open two months later (CFU magnetic station in Fig. 1b). This equipment worked on continuous recording for about 60 days before the eruption started. Unfortunately, the intense fall of volcanic ash on this magnetometer caused damage to the equipment, which stopped working properly soon after the beginning of the eruption. Then, on September 22, 2021, a second magnetometer was installed ~15 km south of the eruptive vents (SAN magnetic station) to work during the whole eruption.

A third magnetometer was deployed on July 22, 2021, in the north of the island, over an extinct stratovolcano, to be used as a complementary reference station (GAR). Due to technical reasons, the data acquired by this equipment in the first two months were extremely noisy and could not be used. The problem was solved just after the beginning of the eruption and data acquired at GAR during the eruptive phase have been used for the reduction of the magnetic series of the SAN magnetic station. The geomagnetic observatory of Güímar (GUI) of the Instituto Geográfico Nacional of Spain (IGN), in the island of Tenerife, was also used as reference for the analysis of all the series (see location in Fig. 1a).

The analysis of these geomagnetic time series and the identification of some possible volcanomagnetic signals are described in the paper.

2. The 2021 Tajogaite volcanic eruption in the Cumbre Vieja Rift on La Palma

The island of La Palma, located in the western part of the Canary Islands (Fig. 1a), is one of the youngest of this volcanic archipelago, with its oldest materials dated at ~1.7 Ma (Carracedo et al., 2001) emplaced over 150 Ma Jurassic oceanic crust (Verhoef et al., 1991). It is a steep-sided, elongated island, measuring ~40 km × 25 km in the N-S and *E*-W directions, respectively, with its highest point reaching 2426 m above the sea level. The present island morphology is the result of a complex alternation of constructive and destructive processes, where two main polygenetic stratovolcanoes can be identified: the northern shield, comprising the Garafía, Taburiente and Bejenado volcanoes, and the southern Cumbre Vieja edifice, which is the site of the present volcanic activity (Ancochea et al., 1994; Carracedo et al., 2001). At least two giant collapses dismantled the northern shield at 1.2 Ma and 560 ky ago. The first one formed the Taburiente caldera, later dismantled by severe erosional processes, where the unusual outcrop of materials pertaining to the early seamount contributed to a better understanding of the initial submarine stages of growth of ocean island volcanoes (Staudigel and Schmincke, 1984).

The Cumbre Vieja rift is a 20 km long, elongated structure in the southern part of La Palma with the shape of a gable roof, resulting from eruptive activity in the last 123 ka along a N-S linear trend that can be easily recognized from the topographic ridge and the alignment of volcanic cones (see Fig. 1c). Historical records report the occurrence of six eruptions in La Palma in 500 years (Hernández-Pacheco and Valls, 1982): 1470–1492 (Tacande), 1585 (Jedey/Tahuya), 1646 (Tigalate), 1677–78 (Fuencaliente), 1712 (El Charco), 1949 (San Juan) and 1971 (Teneguía). All historical eruptions opened vents in the vicinity of the rift axis, with lava fields that run to the sea both eastwards and westwards, as well as southwards in the case of the eruptions placed near the southern end of the rift (Fig. 1c).

The inner structure of the island, obtained from gravity data (Camacho et al., 2009; Montesinos et al., 2023), magnetotelluric sounding (Di Paolo et al., 2020) and seismic tomography (D'Auria et al., 2022; Cabrera-Pérez et al., 2023; Ortega-Ramos et al., 2024) shows a complex pattern beneath Cumbre Vieja. Two low-density bodies are present at both sides of the rift axis at depths between ~the sea level and 4 km b.s.l. Magnetotelluric sounding revealed low-resistivity anomalies in coincidence with those low-density bodies in the same depth range. These results suggest that an active hydrothermal system, where hot volcanic fluids circulate through highly altered and fractured materials, is present beneath the Cumbre Vieja rift flanks down to a depth of ~4 km b.s.l. The estimated lateral boundaries of these structures at a depth of ~3 km b.s.l. are shown in Fig. 1b.

Three levels of magma accumulation have been identified beneath La Palma by means of a geobarometric study of basaltic lavas and mafic to ultramafic xenoliths using thermobarometry and microthermometry of CO2-dominated fluid inclusions (Klügel et al., 2005): a major crystal fractionation level in the upper mantle corresponding to a pressure range 410–770 MPa (15–26 km depth); a short-time stagnation level at the base of the oceanic crust defined by pressures from 240 to 470 MPa (7–14 km depth) that becomes filled before eruptions, where the stagnation time of passing magmas during eruption varies from hours to days; and a shallow intrusion level corresponding to the intrusive core of the island at pressures comprised between 100 and 150 MPa (4–6 km depth). Recent seismic tomography studies have found geophysical evidence of the presence of magma beneath Cumbre Vieja. D'Auria et al. (2022) suggested that a large sub-crustal magma-filled rock volume extends at depths from 7 to 25 km, whereas Ortega-Ramos et al. (2024) interpreted a low velocity zone from 13 km to 37 km depth as a zone of partial melting with interconnected magmatic chambers.

After a quiescence period of 46 years following the Teneguía eruption in 1971, seismic unrest started in October 2017 with the occurrence of a seismic swarm comprising 128 events in 8 days, with mbLg magnitudes between 1 and 2 at depths in the range 20–25 km (Torres-González et al., 2020). A second seismic swarm, with similar characteristics, was detected in February 2018, followed by other eight swarms from June 2020, with the last one occurring on 27–28 August 2021 (IGN, 2022). All these events (October 2017–August 2021) were located at depths in the range 14–35 km, with most of them around 20–25 km, suggesting that an input of fresh magma was arriving to the upper mantle and possibly to the base of the crust beneath the Cumbre Vieja rift. These hypocentral depths are coherent with the deepest level of magma storage identified by Klügel et al. (2005). Geochemical data acquired before and after the first (October 2017) and second (February 2018) seismic swarms revealed changes in the gas emissions of helium, radon and CO_2 related to the circulation of volcanic fluids, suggesting that a reawakening of the Cumbre Vieja volcanic system was taking place (Torres-González et al., 2020).

The volcanic process accelerated by September 11th, when a seismic swarm comprising hundreds of volcanotectonic events, with higher magnitudes than the preceding swarms and decreasing hypocentral depths, revealed that magma was ascending rapidly through the crust (Fig. 2). Eight days later, on September 19th, a fissure opened on the western flank of the Cumbre Vieja rift, approximately 2 km to the northwest of the site of the 1949 historical eruption of San Juan (Fig. 1c). Six major craters and some minor vents were formed, building a 200 m-high composite volcanic cone and lava fields covering an area

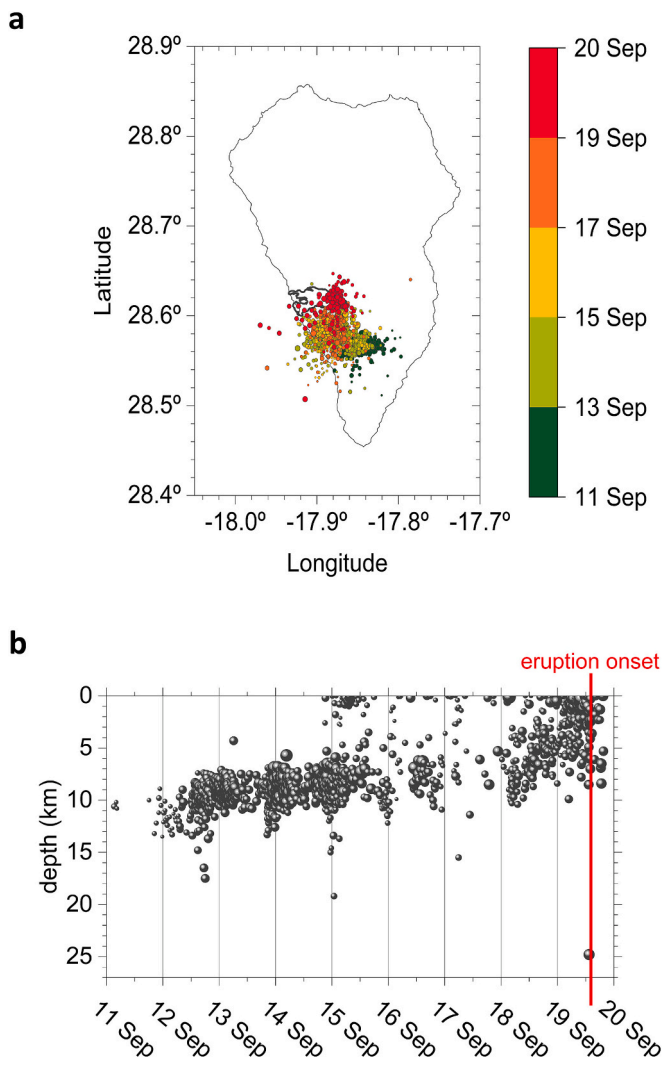

Fig. 2. a) Epicenters of the volcanotectonic earthquakes immediately preceding the 2021 eruption onset, from September 11 to 19. The thick black contour shows the boundaries of the lava field produced by the eruption. b) Hypocentral depths of the same earthquakes. The size of the circles is proportional to the magnitude of the events (IGN, 2022).

of more than 12 km^2, as the result of combined Strombolian and effusive activity that lasted 85 days and was controlled by two faults: the NW-SE trending Tazacorte fault and the ENE-WSW Mazo fault (Rodríguez-Pascua et al., 2024). The eruption ended on December 13, 2021, after the emission of approximately 34 × 10^6 m^3 of lavas of tephritic to basanitic composition (Day et al., 2022) that blanketed and destroyed almost 3000 buildings (IGME, 2021). Compared with historical eruptions in La Palma (Hernández-Pacheco and Valls, 1982; Longpré and Felpeto, 2021) these data make this eruption the most important in the last 500 years in this island in terms of duration, volume of emitted material and damage caused to the local population.

Earlier signs of unrest were suggested by a change in the geochemistry of volcanic fluids in the Cumbre Vieja edifice, with a substantial increase in the CO_2 emission between 2011 and 2013 (Padrón et al., 2015) and changes in the helium isotope ratios from 2008 to 2013 (Padrón et al., 2022). Recently, Fernández et al. (2021) found evidence of unrest from ground deformation detected by reviewing geodetic satellite data in the western flank of the Cumbre Vieja rift, suggesting that a magma injection at ~8–10 km depth took place in 2009–2010.

A ground uplift of 20–25 cm was detected in the vicinity of the emission centre by Differential Interferometric Synthetic Aperture Radar (DInSAR) in the days preceding the eruption (De Luca et al., 2022). In addition, Fernández et al. (2022) analyzed InSAR data and reported, in a selected pixel near the eruptive centre, a moderate deformation of a few cm during nine months prior to the eruption onset.

Different models describing the process of magma ascent in the week preceding the eruption and the geometry of the plumbing system of the new volcano have been recently proposed, based on seismic information (D'Auria et al., 2022; Del Fresno et al., 2023; Suárez et al., 2023), satellite deformation data (De Luca et al., 2022; Fernández et al., 2022; Przeor et al., 2024) and gravity (Montesinos et al., 2023). All models consist of a network of interconnected sills and dykes propagating from the intermediate level of magma storage at the base of the crust to the eruptive fissure, including some aborted branches that did not get to the surface.

3. Magnetic data acquisition and processing

In Fig. 1b we show the location of the three magnetic stations used in this study: CFU was located in the vicinity of the Caños de Fuego visitors center, 2 km away from the 2021 Tajogaite eruptive vents; GAR was situated in the northern part of La Palma island, in a place called Roque del Faro, outside the active volcanic area at a distance of 22 km from CFU station; and SAN was located 13 km to the south of CFU, on the southern end of the Cumbre Vieja rift. The three stations worked with GEM Systems Overhauser magnetometers that acquire the scalar total intensity of the Earth's magnetic field (F) with a sampling rate of 1 measurement per minute and are still in operation today.

In this work we analyzed the geomagnetic time series acquired at CFU from July 23 to September 19, 2021, and those ones acquired at SAN and at GAR from September 23 to December 24, 2021. The geomagnetic observatory of Güímar, GUI, in Tenerife, 145 km away from the CFU station (see Fig. 1a), was used as a reference station.

Identifying eventual volcanomagnetic signals from a total magnetic field registration is a challenging task because the signal must be isolated from a superposition of several time-varying magnetic fields.

Mathematically, we can write the total magnetic field $\mathbf{B}$ at a point P in an active volcano as (Pozzi et al., 1979; Del Negro and Ferrucci, 2000):

$$\mathbf{B}(P,t) = \mathbf{B}_c(P,t) + \mathbf{B}_a(P,t) + \mathbf{B}_t(P,t) + \mathbf{B}_v(P,t) \quad (1)$$

Where $\mathbf{B}_c$ is the main field, originated in the Earth's core, with amplitude around 38,700 nT at La Palma (International Geomagnetic Reference Field, 13th generation, IGRF-13 (Alken et al., 2021), http://www.geomag.bgs.ac.uk/data_service/models_compass/igrf_calc.html); $\mathbf{B}_a$ is the local anomaly field, with amplitudes of several thousand nT in volcanic areas, such as the Canary Islands; $\mathbf{B}_t$ is a transitory field related with the solar magnetic activity, with sources mainly in the ionosphere and in the magnetosphere, which varies in space and time and can reach several tens of nT (up to more than 100 nT in geomagnetically perturbed days); and $\mathbf{B}_v$ is the volcanomagnetic field, that is, the magnetic field (which can be present or not) due to changes in the rocks' magnetization of the volcanic edifice caused by volcanic activity. The amplitude of this field is usually under 15 nT and, depending on the physical mechanism that originates it, its time scale can range from hours to months or even years.

Magnetic fields $\mathbf{B}_c$ and $\mathbf{B}_a$ vary very slowly in time. Therefore, it can be assumed that there is a "background" geomagnetic field at each site, $\mathbf{B}_s$, (resulting from the sum of the constituent fields $\mathbf{B}_c$ and $\mathbf{B}_a$ at that point) that remains almost constant when the studied time series has a duration of a few months. In particular, the secular variation of the main field in the Canary Islands region, estimated by the IGRF-13 model (Alken et al., 2021), was −9.2 nT/year in La Palma and − 11.6 nT/year in Tenerife in 2021. Considering that the maximum duration of our time series is three months, this means that the secular variation will produce a decrease of up to ~2.3 nT in the geomagnetic field measured by our stations in La Palma. Later we will show that neglecting this decrease

does not affect the identification of the volcanomagnetic signals related to the reactivation of Cumbre Vieja.

The "background" geomagnetic field $\mathbf{B}_s$ varies from one station to another in several thousand nanotesla. To make the registrations comparable among them and considering that we are only interested in the temporal variations of the geomagnetic field, we computed the differences respect the mean value of the total magnetic field at each station during the studied time interval. Since scalar magnetometers measure the length of vector **B**, which is usually referred to as *F*, at each station *S*, for each measurement made at instant *t*, we can write:

$$\Delta F_s(t) = F_s(t) - \overline{F_s} \tag{2}$$

where $\overline{F_S}$ corresponds to the mean value of *F* at *S*. This calculation removes the "static" geomagnetic field contributions from the data and is equivalent to subtracting the first two terms in eq. (1).

The next step of the data processing is to separate the temporal variations of the geomagnetic field due to volcanic processes, $\mathbf{B}_v$, from those linked to solar activity, $\mathbf{B}_t$. Two contributions can be identified in the magnetic field $\mathbf{B}_t$: an external field $\mathbf{B}_{te}$, with sources in the ionosphere and in the magnetosphere, and an internal field $\mathbf{B}_{ti}$, which derives from the electrical currents induced by the time-varying field $\mathbf{B}_{te}$ in the conductive structure of the Earth's crust:

$$\mathbf{B_t}(P,t) = \mathbf{B_{te}}(P,t) + \mathbf{B_{ti}}(P,t) \tag{3}$$

The main difficulty for the isolation of a volcanomagnetic signal is that different conductivity structures in the subsoil will generate a different field $\mathbf{B}_{ti}$ at each site for the same inducing field $\mathbf{B}_{te}$. Therefore, depending on the characteristics of the volcanomagnetic field (amplitude and duration), its identification can be obscured by the overlapping of other time-varying geomagnetic signals directly related to the geological structures beneath the station.

Bearing this in mind, our approach consisted of two steps. First, considering that the most important periodic variation of the external magnetic field is the diurnal variation, with main periods at 24, 12 and 8 h (Parkinson, 1983), we have worked with daily-averaged magnetic field values to filter out this variation. It is worth noting that we have tested whether considering only the night-time hours for obtaining the daily average could improve the isolation of magnetic signals not related with solar activity but concluded that the results were not affected by this. Therefore, the daily averages were calculated considering the 1440 measurements of each day (1 datum/min).

Then, we calculated the differences between variations $\Delta F(t)$ defined in eq. 2 for each pair of stations. Thus, for two generic stations *A* and *B* (being *A* the one located in the active volcanic area and *B* the one used as reference station outside the active area) we obtained

$\Delta F_{A-B}(t)$

as:

$$\Delta F_{A-B}(t) = \Delta F_A(t) - \Delta F_B(t) = [F_A(t) - \overline{F_A}] - [F_B(t) - \overline{F_B}] \tag{4}$$

It can be assumed that the external magnetic field $\mathbf{B}_{te}$ behaves very similarly in close stations (within distances of the order of tens of km) and that the directions of the magnetic field vectors are close enough to enable making calculations with their lengths. This implies that the computation of the differences $\Delta F_{A-B}(t)$ practically removes the low-frequency magnetic fields originated outside the Earth that still remain in the data after the calculation of the daily average values and, for that reason, this calculation is usually carried out in the data processing of volcanomagnetic studies (i.e. Zlotnicki and Bof, 1998; Del Negro et al., 2004; Kanda, 2010). Therefore, considering that transient magnetic fields linked to volcanic activity can only be present in the station situated in the active volcanic area (*A*), the residual field $\Delta F_{A\text{-}B}(t)$ would basically contain: a) the differences between the local induced magnetic fields at both sites; and b) the volcanomagnetic signals in *A*, in case they exist; both with periods longer than one day, since we are working with daily-averaged values. It is expected that the first of these contributions is enhanced on days of intense solar activity. For that reason, the external geomagnetic field behavior, quantified through the K-index values, was taken into account for the identification of eventual volcanomagnetic signals. At each geomagnetic observatory, K-indices quantify how far the variations of the magnetic field are from a standard magnetically quiet day at that site (Parkinson, 1983). They are calculated for three-hour periods. Therefore, eight values of K-index ranging from 0 to 9 are obtained for each day. To visually analyze possible correlations between the residual magnetic field $\Delta F_{A\text{-}B}(t)$ and external geomagnetic field variations we calculated the sum of the eight values of the K-index at the Güímar geomagnetic observatory for each day and plotted them in the figures.

In the Results section we will show that this approach was efficient for isolating at least one magnetic signal probably related to the recent volcanic activity of Cumbre Vieja.

4. Results

In Fig. 3 we show the geomagnetic field total intensity (*F*) time series acquired at magnetic station CFU in La Palma and at Güímar geomagnetic observatory in Tenerife (GUI) in the two months preceding the eruption onset, from July 23 to September 19, 2021. The figure also displays the magnetic activity index K at the Güímar geomagnetic observatory for the same dates. It can be noted that the greatest amplitude variations of *F* at both sites occurred on days with the highest values of K, around August 27–28 and September 17. Other dates when solar activity was intense were July 28, August 2, and September 7–8. All those days are marked with arrows in Fig. 3 to warn the reader that magnetic field variations from station to station on those dates would be probably related to external geomagnetic activity rather than to volcanic activity.

In Fig. 4a we show the difference between the daily mean value of *F* and the average value of *F* from July 23 to September 19, 2021 (ΔF in eq. 2) for the CFU station and for the GUI observatory in Tenerife. In addition, the magnetic field residuals obtained by subtracting the ΔF values measured at GUI from those measured at CFU ($\Delta F_{CFU\text{-}GUI}$) are displayed in Fig. 4b, where the time derivative of this residual field is superimposed to illustrate its evolution in time.

It can be noted that the residual field $\Delta F_{CFU\text{-}GUI}$ remains practically constant with slight variations from the beginning of the series until about August 8 (day 220 in Fig. 4). Then, it decreases about 3 nT from August 8 to August 13 (day 225). Around that date, the residual field starts a rapid increase of approximately 10 nT in four days, ending by August 17 (day 229). From August 18 (day 230), it starts decreasing for five days until August 23 (day 235). Looking at the K-index pattern (Fig. 4c) it can be noted that nor the rapid increase of the residual field neither its subsequent decrease is correlated with the occurrence of any particularly high external geomagnetic activity. From August 23 until the eruption onset, the residual field shows small positive and negative variations, always below 2–3 nT.

Based on this pattern, we propose that a magnetic signal of volcanic origin, with an amplitude of approximately 10 nT, is revealed at the CFU station at least from August 13 to 23, nearly one month before the beginning of the eruption. We tentatively distinguish three different phases in this signal, which are highlighted with different colors in Fig. 4: a rapid increase of the residual magnetic field (August 13–17, shadowed in light yellow), a brief time interval when the residual field remained almost constant (August 17–18, shadowed in light orange) and a decrease of the residual magnetic field (August 18–23, shadowed in light yellow). A shift of approximately 3 nT seems to be present in the data from August 23 (marked with the dashed, horizontal orange lines), suggesting that the magnetic field had increased in 3 nT permanently after the occurrence of the anomalous event. The time interval from August 8 to 13 is also highlighted in Fig. 4 (light sky blue) because a

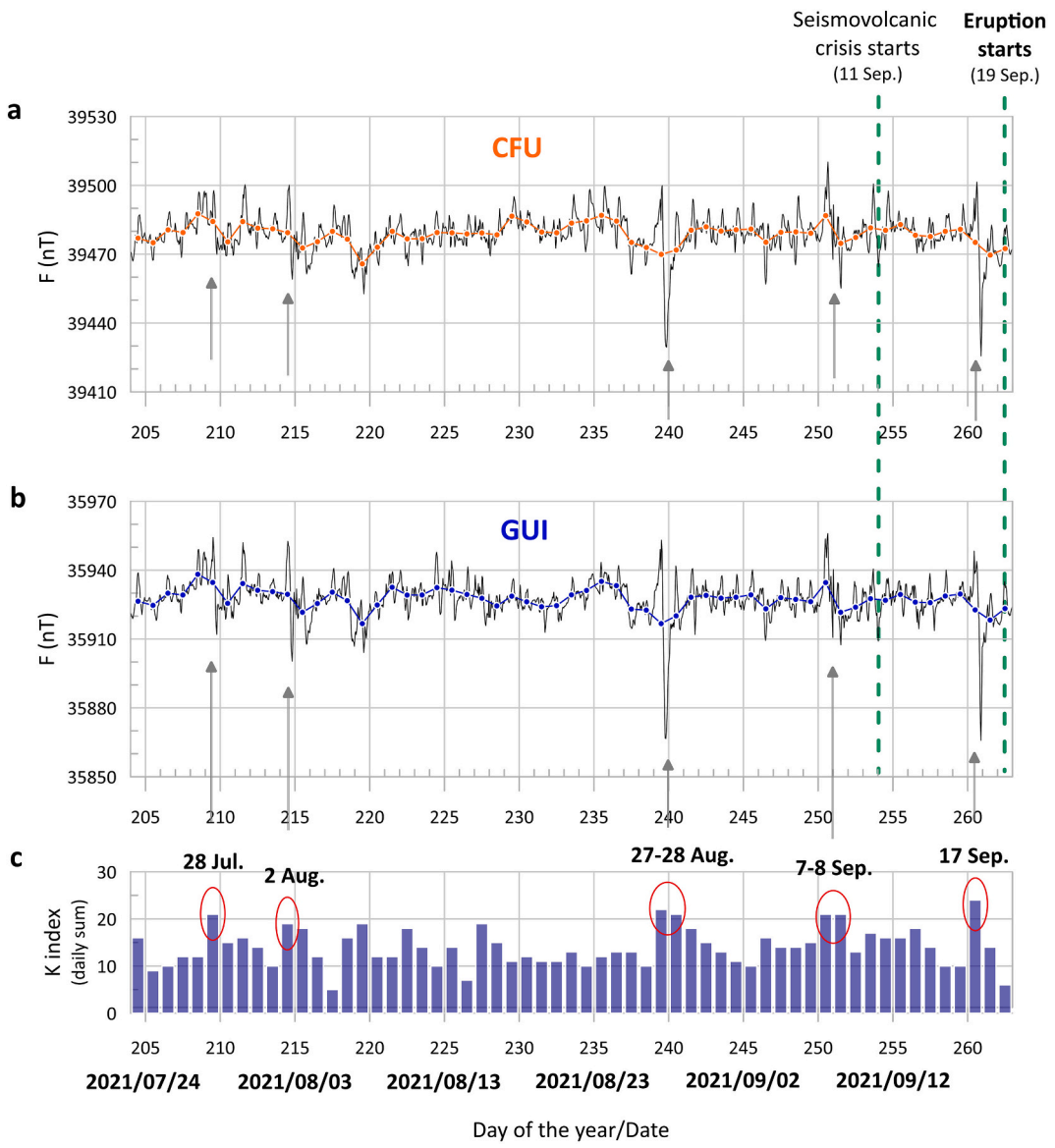

Fig. 3. Geomagnetic field total intensity (*F*) time series acquired at CFU magnetic station in La Palma (a) and at the Güímar geomagnetic observatory, GUI, (b) from July 23 to September 19, 2021. At each station, the black, continuous line shows the hourly mean values, whereas the dotted, coloured line displays the daily mean values. The location of the stations is shown in Fig. 1. The external field magnetic activity index K at the GUI geomagnetic observatory for the studied time interval is also shown (c). The grey arrows point to days with high values of K-index that produced high-amplitude variations of *F* related to solar activity.

decrease in the residual field for some days, preceding the rapid increase starting on August 13, might also be a part of the same magnetic signal.

In addition, around the date when the pre-eruptive seismic started (September 11) the residual field $\Delta F_{CFU\text{-}GUI}$ slightly increased compared to previous values. This would suggest that the triggering of the seismic crisis associated to the rapid magma ascent to the surface could somehow have affected the geomagnetic field at CFU, although this correlation must be interpreted with caution.

We also analyzed the geomagnetic time series acquired at SAN and at GAR magnetic stations from September 23 to December 24, and compared them with the data acquired at the GUI geomagnetic observatory. This time interval spans the duration of the Tajogaite eruption almost entirely (the registration started four days after the beginning of the eruption – September 19 – and stopped eleven days after its end, on December 13). Due to technical issues, there is a gap in the SAN series from October 16 to 23.

In Fig. 5 we show the registration at the three sites, both as hourly mean values and daily mean values of the total field geomagnetic intensity, *F*. Again, the geomagnetic activity index K for the studied time interval is also shown to identify days of high external field variations. It can be noted that several peaks of intense external geomagnetic activity were present in the three months considered.

In Fig. 6a, we show the difference between the *F* daily mean value and the $\overline{F}$ average value calculated from September 23 to December 24 (ΔF in eq. 2) for the SAN and GAR stations in La Palma and for the GUI geomagnetic observatory. It can be noted that the three curves show very similar patterns during the whole period. Fig. 6 also shows that the amplitude of the variations of the residual magnetic field is lower for $\Delta F_{SAN\text{-}GUI}$ than for $\Delta F_{SAN\text{-}GAR}$ and $\Delta F_{GAR\text{-}GUI}$. This must be due to a different site response of the local conductivity structure to the external magnetic field variations at GAR.

It can also be noted that an apparent decrease of a few nT coincides with the end of the eruptive process. From December 13, the magnetic field at SAN is slightly shifted down with respect to GUI and GAR (Fig. 6a). This can be seen in the residual fields $\Delta F_{SAN\text{-}GUI}$ (Fig. 6b) and $\Delta F_{SAN\text{-}GAR}$ (Fig. 6c), which decreased from that date and turned negative,

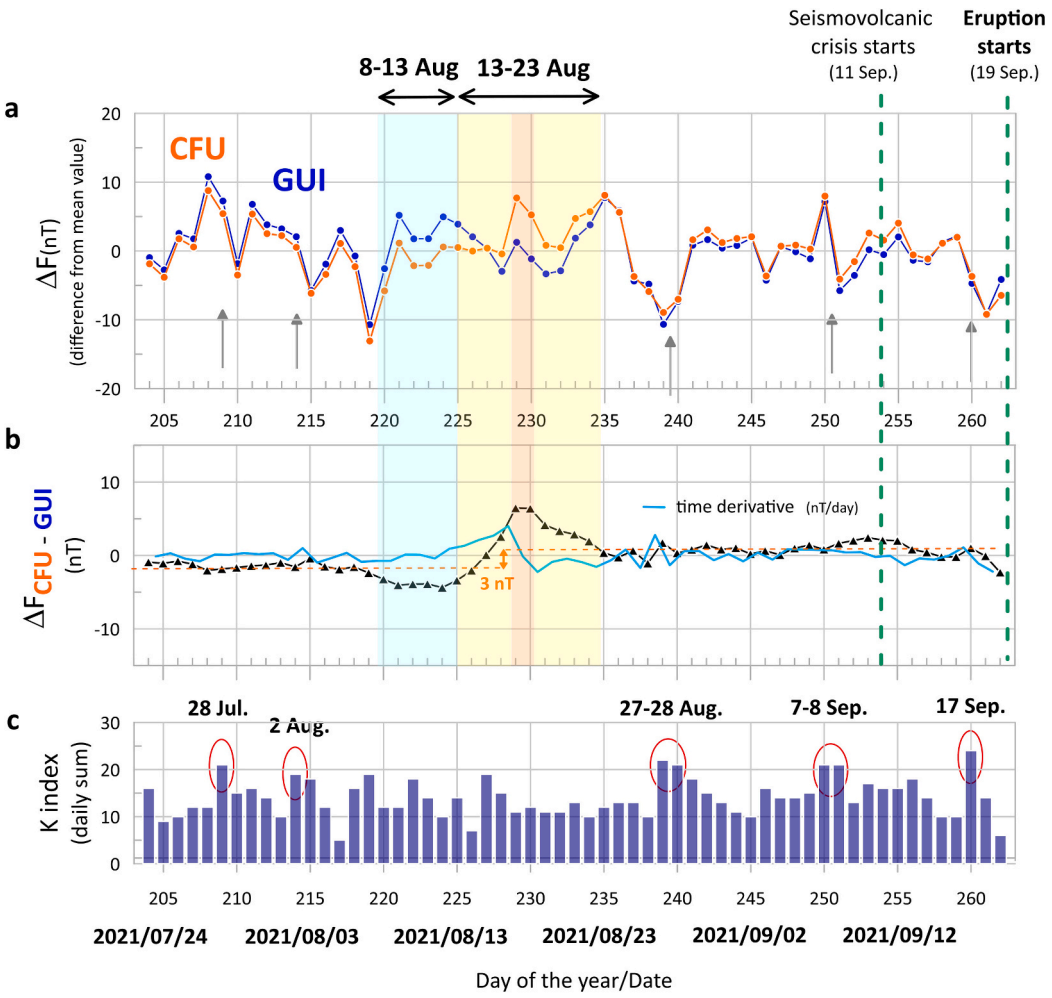

Fig. 4. a) Difference between the *F* daily mean value and the average of *F* from July 23 to September 19, 2021 (*ΔF* in the text) for the CFU station (orange) and for the GUI geomagnetic observatory (blue). b) Geomagnetic field residuals obtained by subtracting the *ΔF* values at GUI from those measured at CFU. The time derivative (light blue line) is superimposed to illustrate the evolution of the residual field. A magnetic signal, with amplitude of approximately 10 nT, is revealed at CFU at least from August 13 to 23, where three different phases are enhanced with different colour shadowing (see the text). A shift of ~3 nT seems to remain in the residual field after that date (dashed, horizontal orange lines in the figure). From August 8 to 13 (highlighted in light sky blue) the decrease of the residual field might also be a part of the same magnetic signal. c) External field magnetic activity index K at the GUI geomagnetic observatory for the studied time interval. The grey arrows point to days with high values of K-index that produced high-amplitude variations of *F* related to solar activity. (For interpretation of the references to colour in this figure legend, the reader is referred to the web version of this article.)

compared with the previous values. However, no signal can be identified in the residual field $\Delta F_{GAR\text{-}GUI}$ (Fig. 6d) for the same period. This suggests that the magnetic field at SAN could be reflecting the end of the volcanic activity.

5. Correlation with other physical parameters

5.1. Ground deformation

The intrusion of magma at depth is usually accompanied by ground deformation in the surface and therefore geodetic monitoring is a classical tool used for eruption forecasting in active volcanoes (i.e. Dzurisin, 2003; Sparks, 2003; Sigmundsson et al., 2022).

In the case of La Palma, we have compiled existing information on ground deformation just before the 2021 eruption and have supplemented it with information obtained from new analysis of GNSS data.

We examined in detail the results previously reported by other authors on the ground deformation immediately preceding the eruption. By August 25, a slight jump is noted (see Fig. 3 of De Luca et al., 2022) in the deformation pattern registered at GNSS stations LP03 and LP04, located on the western flank of the Cumbre Vieja edifice, 3 km to the south of the CFU station (Fig. 1b). Additionally, analysis of Sentinel-1 data from September 2020 to October 2021 revealed that uplift in the vicinity of the (future) eruptive vents began to increase by mid-August 2021 (Benito et al., 2023) and accelerated by the end of that month (Lekkas et al., 2021).

We calculated the baseline change using public GNSS data available from IGN and GRAFCAN (LP01, LPAL, and MAZO stations shown in Fig. 1b) for the period that coincides with our magnetic records at CFU station, from July 23 to September 24 (Fig. 7a). Apart from the evident baseline alteration produced in correspondence with the pre-eruptive, September 11–19 seismic swarm, it can be noted that the baseline LP01-MAZO presents a remarkable change (~ 5 mm) during August 13–24, that is, one month before the beginning of the eruption and coinciding with the magnetic signal of ~10 nT detected at CFU (see Fig. 4). Also, the LPAL-MAZO baseline displays variations up to 4 mm in this period. In more detail, the baseline analysis shows that LPAL was the most stable among the three stations from 13 to 24 August, with maximum variations in the horizontal coordinates of 2 mm and 1 mm in the N-S and *E*-W directions, respectively. In the same days, LP01 varied up to 6 mm and 2 mm in the E-W direction while MAZO varied up to 3 mm in the same direction. Regarding the N-S direction, both LP01 and

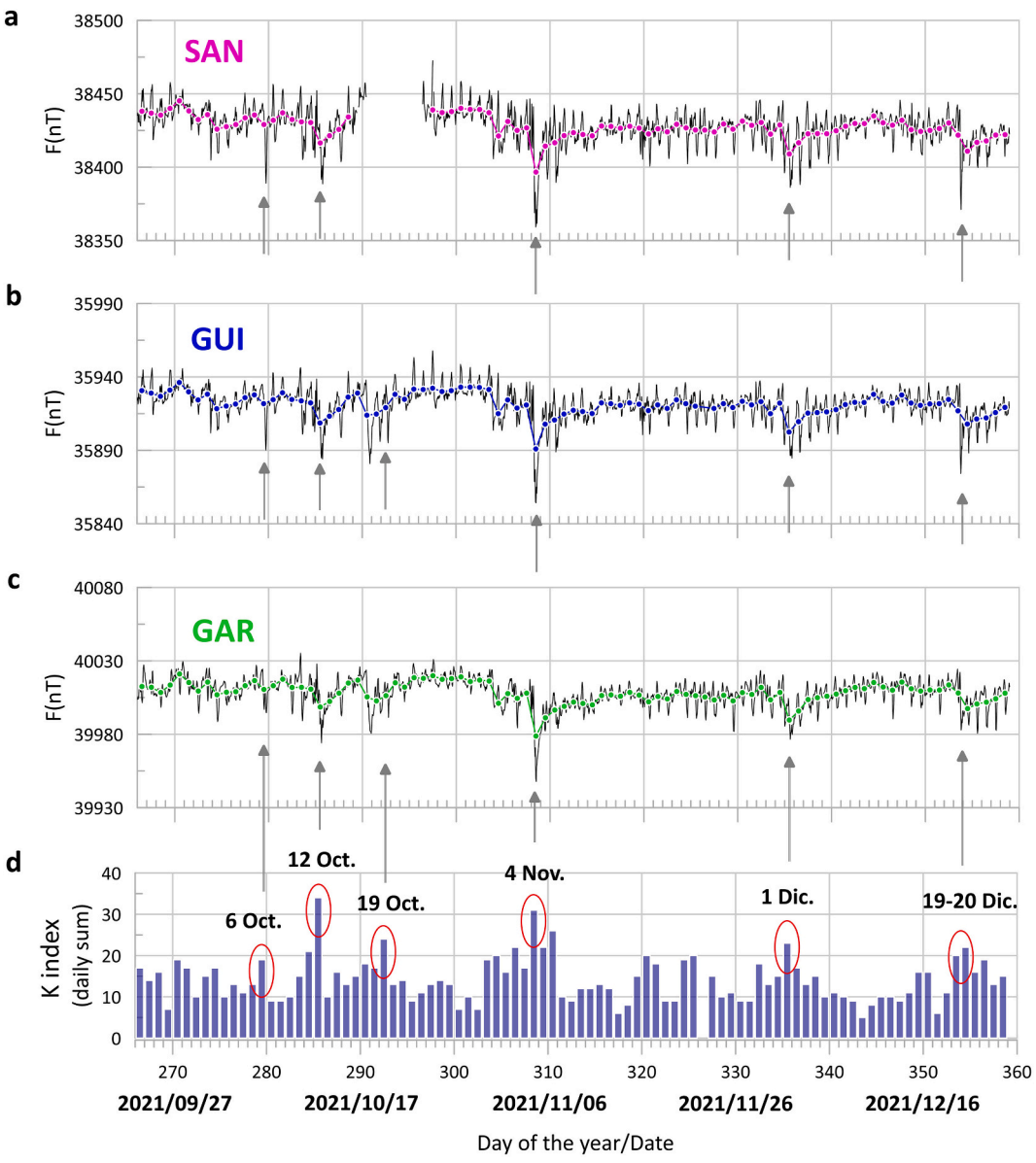

Fig. 5. Geomagnetic field total intensity (*F*) time series acquired at SAN magnetic station (a), at GUI geomagnetic observatory (b), and at GAR magnetic station (c) from September 23 to December 24, 2021. The location of the stations is shown in Fig. 1. In each plot, the black, continuous line shows the hourly mean values, whereas the dotted, colored line displays the daily mean values. The external field magnetic activity index K at GUI geomagnetic observatory for the studied time interval is also shown (d). The grey arrows point to days with high values of K-index that produced high-amplitude variations of *F* related to solar activity.

MAZO show maximum variations of 2 mm from 13 to 24 August.

In the week preceding the eruption onset, the main deformation identified by satellite studies affected the southern portion of the Cumbre Vieja rift (De Luca et al., 2022; Fernández et al., 2022; Przeor et al., 2024). LP01 and MAZO stations are close to this area. Therefore, it is likely that the baseline variations observed in August were due to a shallow ground deformation in the vicinity of LP01 and MAZO stations.

5.2. Seismicity

In active volcanoes, a great variety of seismic events can be observed. Attending to the physics of the source, two families of processes can be defined: volumetric sources, where fluids (volcanic or geothermal) play a role on the generation of the elastic waves (long period events and volcanic tremor) and shear or tensile sources involving brittle rock failure (volcanotectonic events) (Chouet, 1996).

Long-period (LP) events show a characteristic signature consisting of a high-frequency onset followed by a harmonic waveform containing one or up to several dominant periods in the range of 0.2–2 s. When periods are larger than 2 s, they are referred to as very-long-period (VLP) events. This signature is commonly interpreted as oscillations of a fluid-filled resonator (cavity or crack) in response to a time-localized excitation. This kind of seismicity reflects pressure fluctuations resulting from unsteady mass transport in the sub-surface plumbing system that, when occurring at shallow depths, may be a useful indicator of impending eruption (Chouet, 1996, 2003). In fact, several important eruptions have been preceded by precursory LP events, such as the cases of Asama volcano in Japan (1958 and 1983), El Chichón in Mexico (1982), Redoubt in Alaska (1989–90), Mt. Pinatubo in Philippines (1991) and Galeras in Colombia (1993) (Chouet, 1996 and references therein). The study of LP and VLP events has considerably increased in the last decades due to the generalized use of broadband seismometers for volcano monitoring.

In the three months preceding the eruption onset, the most

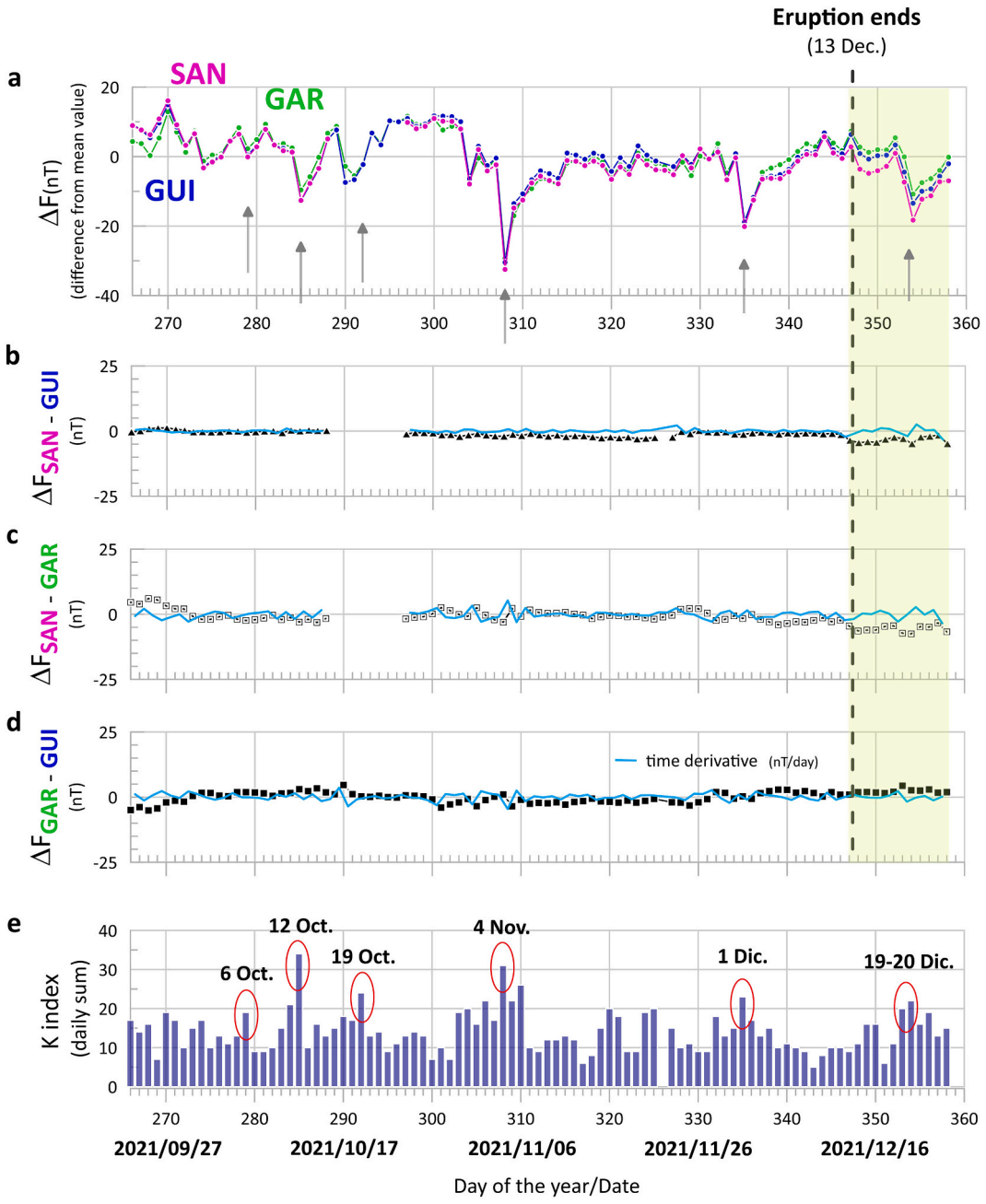

Fig. 6. a) Difference between the *F* daily mean value and the average of *F* from September 23 to December 24, 2021 (*ΔF* in the text) at SAN (magenta) and GAR (green) stations and at GUI geomagnetic observatory (blue). b) and c) Geomagnetic field residuals obtained by comparing the *ΔF* values at SAN with those measured at GUI and at GAR. The time derivative (light blue line) is superimposed to illustrate the evolution of the residual fields. An apparent decrease of a few nT coincides with the end of the eruptive process (shadowed in light green). d) Residual field obtained by subtracting the *ΔF* values at GUI from those measured at GAR. e) External field magnetic activity index K at GUI geomagnetic observatory for the studied time interval. The grey arrows point to days with high values of K-index that produced high-amplitude variations of *F* related to solar activity. (For interpretation of the references to colour in this figure legend, the reader is referred to the web version of this article.)

remarkable volcanotectonic (VT) seismic activity (excluding the pre-eruptive September 11–19 seismic swarms) were two swarms that occurred on June 25–27 and on August 27–28, respectively. The first one comprised 37 VT events with magnitudes from 0.9 to 2.2 m_{bLg} at depths around 30 km, whereas the second consisted of 10 events with magnitudes from 0.9 to 1.4 m_{bLg} at depths around 23 km (IGN, 2022). In Fig. 7b and c we show the seismicity in the period from July 23 to September 19, coinciding with our geomagnetic data at CFU station. It is worth noting that the second seismic swarm mentioned before (August 27–28) occurred just a few days after the end of the magnetic signal.

In addition, we have paid especial attention to the occurrence of LP and VLP events in the months preceding the eruption onset to search for eventual correlations with the geomagnetic field. We analyzed public data acquired by 12 seismic stations of the Spanish IGN (see locations in Fig. 8a) that are equipped with three-component broadband seismometers with sample frequency of 100 Hz. We used a seismic catalogue that starts on 22 July 2021 (coinciding with the beginning of the geomagnetic time series acquired at CFU station) and ends on 10 September 2021 (just before the pre-eruptive seismic crisis initiated). Waveforms from all the operating stations are available from the Spanish Digital Seismic Network (IGN, 1999). The waveform data were sub-sampled from 100 Hz to 50 Hz and detrended. Then, the instrument response

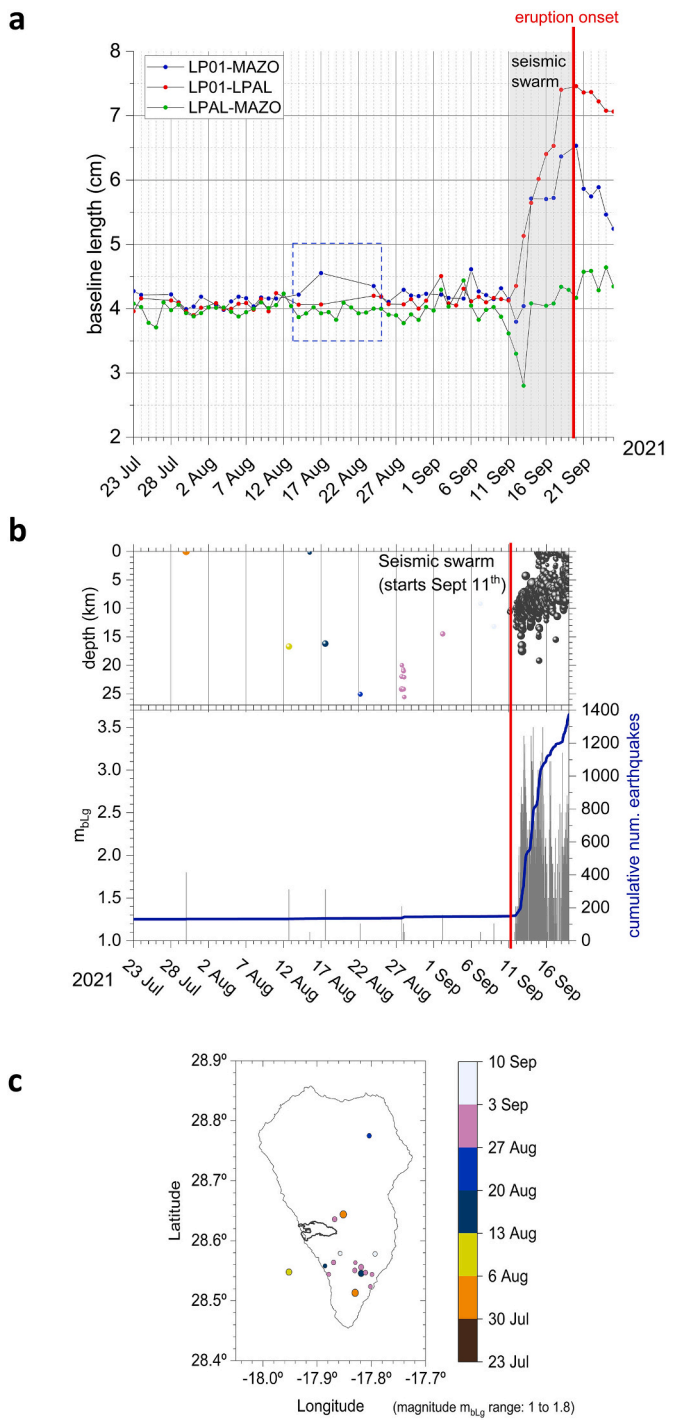

Fig. 7. a) Changes in the baseline length between GNSS stations LP01, LPAL and MAZO (see locations in Fig. 1b) from July 23 to September 24, 2021. The dashed, blue square identifies the period August 13–23 when the magnetic signal was detected. b) Depth, magnitude (mbLg >1) and cumulative number of seismic events recorded from July 23 to September 19, 2021 (IGN, 2022). c) Epicenter location of the seismic events reported in b). (For interpretation of the references to colour in this figure legend, the reader is referred to the web version of this article.)

was removed to obtain ground velocities. All seismic recordings were band-pass filtered at 0.01–1 Hz (1–100 s) to isolate the most energetic part of the recorded LP and VLP events. To easily identify the LP and VLP events, a spectrogram was obtained from the waveforms. Data processing was carried out using SAC (Seismic Analysis Code) (Goldstein et al., 2003; Goldstein and Snoke, 2005). Fig. 8b shows an example of two different waveforms corresponding to some of the detected events. It can be noted that LP events are characterized by a shorter duration and a higher frequency than VLP events. VLPs have a peak frequency at ~0.06 Hz, whereas LPs' peak frequency is ~0.5 Hz. The waveforms of the detected events display similar patterns in terms of period, shape, and duration from station to station.

A total of 30 events (14 LP and 16 VLP) were identified during the studied time interval (Fig. 9). It can be noted that the temporal distribution of the events is not regular. Instead, a clear concentration of both LP and VLP events is found between 11 and 22 August 2021 when 24 of the 30 events occurred, in close correlation with the volcanomagnetic signal identified at the CFU station.

6. Discussion

Although the isolation of transient magnetic fields related to volcanic activity is a delicate issue, our data reduction approach has allowed to identify a presumed volcanomagnetic signal one month (August 13–23) before the 2021 eruption onset in the Cumbre Vieja rift. The change in the rocks' magnetization that produced this signal at the CFU station seems to have caused a permanent shift of +3 nT (see Fig. 4b) on the background value of the geomagnetic field, although this result must be considered with caution due to the limited length of the time series. In the days preceding the triggering of the pre-eruptive seismic crisis (September 11) the magnetic field at CFU seems to have slightly increased, suggesting that a volcanomagnetic signal linked to the impending eruption could also be present around that date. In addition, the end of the volcanic process appears to be correlated with a slight decrease in the geomagnetic field at the SAN station (Fig. 6).

Analyzing the residual field obtained by subtracting the magnetic fields measured at two sites located outside the active area (GAR station in northern La Palma and GUI magnetic observatory in Tenerife) from September 23 to December 24 ($\Delta F_{GAR\text{-}GUI}$ in Fig. 6d), where only the difference in the magnetic field induced by the external magnetic variations must be present ($\mathbf{B}_{ti}$ in Section 3), it can be concluded that variations due to a different conductivity structure beneath these two sites are of the order of a few nT (mean value: 0.03 nT, standard deviation: 2.14 nT). Based on this, it can be deduced that a variation of the order of 10 nT in the residual fields between a station situated in the active volcanic area and a reference station outside it, such as the one identified at the CFU station by mid-August, is significantly higher than the expected amplitude of the difference in the induced magnetic fields. Therefore, it is reasonable to identify it as a magnetic variation of volcanic origin. With this perspective, we will center our discussion on this signal since the amplitudes of the other two (a slight increase of the residual magnetic field at CFU station shown – Fig. 4 – coinciding with the beginning of the eruption, and a slight decrease of the residual magnetic field at SAN station – Fig. 6 – by the end of the eruptive process) are close to the estimated average differences ascribed to a different site response to external geomagnetic variations. Therefore, their identification is not straightforward.

Moreover, the residual field $\Delta F_{SAN\text{-}GUI}$ (Fig. 6b) remained almost constant even in days with high external geomagnetic activity. Therefore, it can be concluded that using the Güímar magnetic observatory as a reference station for the geomagnetic data acquired at stations located in the active Cumbre Vieja volcanic area provides us with high quality and attainable results for the identification of volcanomagnetic signals.

For interpreting possible signals precursory of an eruption, a multiparametric approach is necessary. With that aim, we searched for correlations among our magnetic data and other physical parameters, as we explained in section 5. We found that both published InSAR results (Lekkas et al., 2021; De Luca et al., 2022; Benito et al., 2023) as well as GNSS data (this work, see Fig. 7a) revealed a remarkable ground uplift by mid-August 2021, one month before the eruption, in close coincidence with the magnetic signal observed at the CFU station. Regarding seismicity, we identified a considerable number of LP and VLP events in

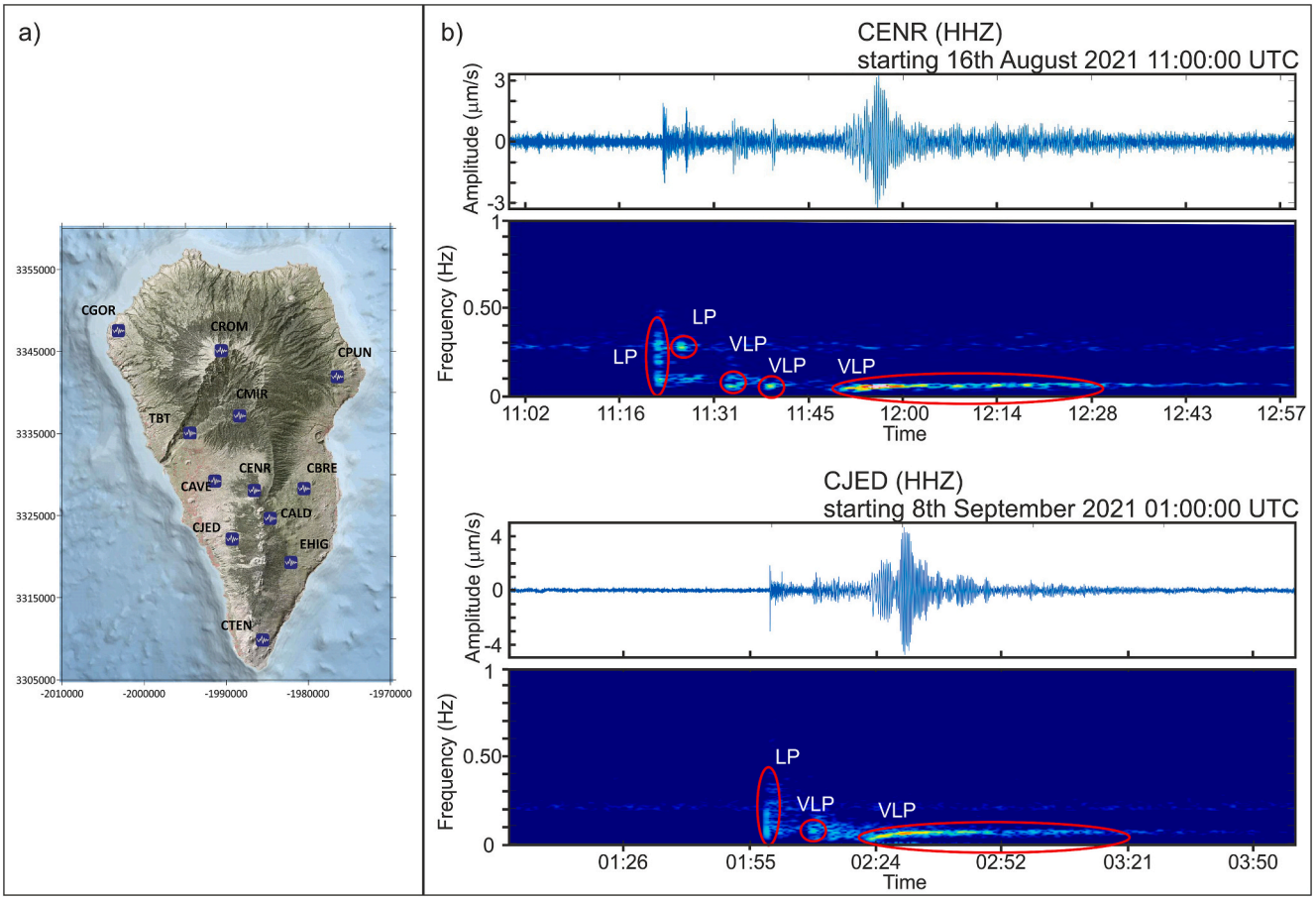

Fig. 8. a) Spatial distribution of the seismic stations belonging to the monitoring network in La Palma (IGN). b) Waveforms and spectrograms of selected events: Two LP events and three VLP events, from 16 August 2021, station CENR (upper pane); one LP event and two VLP events, from 8 September 2021, station CJED (lower pane).

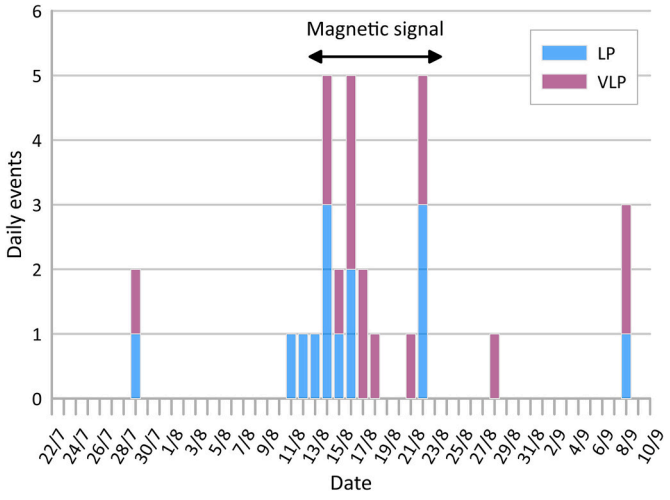

Fig. 9. Histogram showing the daily event count of LP and VLP events recorded from July 22 to September 10, 2021. The time interval of the magnetic signal observed at the CFU station is indicated (August 13–23).

the two months preceding the eruption onset with a temporal distribution that clearly points to mid-August as a moment of intense LP and VLP seismic activity (see Fig. 9).

In addition, Benito et al. (2023) analyzed radiance images acquired by NASA Advanced Spaceborne Thermal Emission and Reflection Radiometer (ASTER) sensor in April 2017 and July 2021 and identified strong thermal spectral anomalies in Cumbre Vieja between those dates, especially in the area where the volcanic vents would open in September 2021. This suggests that heat from deep magmatic intrusions had already arrived at the surface at least two months before the onset of the eruption.

All these results provide us with evidence of an event with a duration of 10–15 days by mid-August that should have changed to some extent the physical state of the pre-eruptive volcanic system at shallow levels.

Basically, three physical mechanisms can account for magnetic field variations related to volcanic activity (Johnston, 1997): thermomagnetism, or variations of the magnetic field due to temperature variations of the rocks; piezomagnetic effects, or magnetic field variations related to changes in the stress field beneath the studied area; and electrokinetic processes, which produce changes in the local magnetic field linked to alterations in the hydrothermal system due to volcanic activity. In most occasions, volcanomagnetic variations are due to more than one of these phenomena acting together.

The duration and amplitude of transient magnetic fields observed in active volcanoes can help us deciphering what is the physical mechanism that produced them. Volcanomagnetic anomalies of pure thermal origin are usually long-term signals that can last for months or years and can reach several tens of nT (i.e. Yukutake et al., 1990; Del Negro and Ferrucci, 1998). They can be observed when new melted material (demagnetized) is emplaced at shallow depth or when a cooling intrusion progressively acquires a thermoremanent magnetization. The sign (positive or negative) of the observed signal will depend on the loss/acquisition of magnetization and on the relative position of the magnetic

station with respect to the source of the anomaly. The volume affected by demagnetization/magnetization is usually small and therefore thermomagnetic signals are only detectable when the magnetic field is measured very close to the sources. This also implies that the intrusion must be shallow to be able to affect the magnetic field measured on the surface. A rock magnetic study carried out with samples from lava flows and pyroclastic deposits erupted in Cumbre Vieja (Parés et al., 2022) showed that the main magnetic mineral was Ti-rich titanomagnetite, characterized by low to medium unblocking temperatures. This means that at temperatures as low as ~200 °C, most of the magnetization can be erased from the rocks.

Conversely to thermomagnetic anomalies, volcanomagnetic signals of piezomagnetic or electrokinetic origin are usually characterized by much shorter time scales. Piezomagnetic effects (Stacey et al., 1965; Sasai, 1980) are related to stress-induced changes in the magnetization of rocks caused by intrusion of magma at depth. The modification of the stress field derived from magma intrusion may have a mechanical or a thermal origin due to hydrothermal pressurization that can propagate fast and far from an intrusion as a transient phenomenon (Delaney, 1982; Okubo and Kanda, 2010). When a clear correlation between the occurrence of seismic swarms and volcanomagnetic signals is detected, considering a piezomagnetic origin for those signals becomes straightforward (Currenti et al., 2007; Napoli et al., 2008).

When an active hydrothermal system is present beneath the volcanic edifice, electrokinetic effects can produce a detectable magnetic field if changes in the circulation of fluids within the interconnected crack and fissure networks occur. These effects are related with the presence of an electric double layer at the solid-liquid interface, with separated positive and negative ions, that creates an electric potential (streaming potential) controlled by pore-pressure gradients (Fitterman, 1979, 1981). For instance, in Piton de la Fournaise volcano (Réunion island), electrokinetic effects appeared to be the main mechanism generating volcanomagnetic signals up to 15 nT (Zlotnicki and Le Mouel, 1988; Zlotnicki et al., 1993).

Magmatic reactivation is a complex phenomenon that starts at depth involving several physical processes that can contemporarily produce changes at shallow levels. Associated high-temperature fluids might transport heat from the magmatic body to shallow depths. These effects are enhanced when an active hydrothermal system exists, because heat transfer by fluids through pores and cracks is more efficient and rapid than conduction.

In Cumbre Vieja, the presence of an active hydrothermal system beneath both flanks of the rift is supported by geophysical evidence (Di Paolo et al., 2020). In the western flank, the volume affected by alteration and fracturing is 15 km long and 5 km wide (see Fig. 1b), with its top at ~2 km and its bottom at ~4 km. The CFU magnetic station is located over this body, whereas the SAN magnetometer is located very close to its southern end. All this area has been affected by seismic activity in the pre-eruptive phase since the beginning of the seismic unrest in 2017 (Torres-González et al., 2020). Regarding diffuse gas emissions, Padrón et al. (2022) analyzed $^{3}He/^{4}He$ ratio data from 1991 to 2021 measured at Dos Aguas mineral spring located at the bottom of the Taburiente caldera (outside the Cumbre Vieja edifice). These authors found that the most recent increase in ^{3}He of magmatic origin took place in the second half of 2020, pointing to a pulse of magma intrusion at depth at that moment. From March 2021 to July 2021, values of the $^{3}He/^{4}He$ ratio were also larger than the average of the period 1991–2021 (see Table S1 and Fig. 4 of the cited paper), probably showing that magmatic fluids were ascending through the crust in those months.

The transient magnetic signal detected at the CFU magnetic station in August suggests that some abrupt change in the volcanic system, capable of affecting the magnetization of rocks at shallow levels, took place one month before the eruption onset.

Volcanotectonic seismic activity was practically absent in this period (see Section 5). In turn, a significant number of LP and VLP events concentrated around mid-August (see Fig. 9), revealing that magmatic and geothermal fluids at shallow depths were being affected by magma intrusion. Among the physical mechanisms that can generate VLP events we can mention the inflation and deflation of magma chambers and cracks and the movement of gas slugs through conduits (Konstantinou, 2024). In hydrothermal systems, a common LP excitation mechanism involves surges in the heat transfer from an underlying magma body that increases pressure in a steam-filled fracture to a critical threshold. Then, an abrupt opening of a pathway allows gas to escape suddenly, initiating a rapid pressure loss, collapse of the fracture, and attendant resonance of the fluid remaining in the fracture (Chouet and Matoza, 2013).

The coincidence in time of significant LP and VLP seismic activity and the observed magnetic signal led us to the conclusion that these phenomena were interrelated. We consider that the hydrothermal system played a crucial role in the generation of the volcanomagnetic signals observed in Cumbre Vieja, which are probably due to more than one physical mechanism acting together. Although hydrothermal systems can significantly enhance heat transport and accelerate thermal demagnetization effects, the time scale of the observed geomagnetic variations (1–2 weeks) suggests that a combination of electrokinetic and piezomagnetic effects is probably causing most of the changes in the rocks magnetization responsible for the detected volcanomagnetic signals.

7. Conclusions

The 2021 volcanic eruption in La Palma Island has provided the scientific community with a unique opportunity of observing and monitoring in real-time a subaerial volcanic eruption for the first time in the Canary Islands. Thanks to this, a fresh wealth of knowledge acquired during the whole reactivation process can be now analyzed for improving our understanding of the present and future Canarian volcanism, with important implications in the hazard assessment.

This work shows that measuring the geomagnetic field could provide additional constraints on the changes in the thermal and stress state of a volcanic system during reawakening, therefore completing models based on ground deformation, seismic activity, and volcanic gas emissions. This could be especially valuable in volcanic environments such as the Canary Islands, where quiescence periods last several decades and eruptive processes can evolve very rapidly, such as in the case of the 2021 eruption in La Palma.

Our results suggest that the volcanic processes related to the 2021 eruption could have caused a significant change in the geomagnetic field before the eruption started at a site located in the area affected by the renewed activity. Even when just one magnetometer was deployed, the data reduction based on the comparison with the geomagnetic field recorded at the Güímar geomagnetic observatory in Tenerife has allowed to successfully isolate a signal of probable volcanomagnetic origin.

This work is based on fresh data (geomagnetic time series and broadband seismic recordings not analyzed in previous papers, as well as surface deformation results) dealing with the reactivation of the Cumbre Vieja volcanic system, which makes it especially valuable. Moreover, this is the first time this type of process can be recorded and identified in Spanish active volcanic areas.

Considering that the detected volcanomagnetic signal probably derived from the complex interplay of several physical mechanisms and that geomagnetic data were available at just one station, a realistic quantitative modelling is not attainable in this case, since too many constraints are missing. Despite this, the qualitative interpretation of the pre-eruptive signal provided us with valuable information about the evolution of the volcanic system several weeks before the beginning of the eruption, while other typical precursors (such as volcanotectonic seismic activity) did not evidence that an eruptive process was forthcoming.

Therefore, we propose that, nearly one month before the eruption,

some abrupt change in the volcanic system occurred. Probably, the overpressure caused by magma intrusion at depth propagated efficiently upwards, through the materials affected by the hydrothermal system, favored by the network of cracks and fissures already present. In addition, hot magmatic gases and fluids associated to this process ascended to the shallowest part of the volcanic edifice through the fracture system, possibly altering the thermal state, the stress field, and the streaming potential. This hypothesis is supported by the occurrence of a significant number of LP and VLP seismic events around mid-August related to movement of pressurized fluids along fractures. As a result of this, the geomagnetic field changed by about 10 nT in the vicinity of the future eruptive vents. Therefore, our results suggest that changes in the volcanic system can affect large portions of the volcanic edifice and modify the rocks magnetization, anticipating changes in other physical or geochemical parameters during a reactivation process.

CRediT authorship contribution statement

Isabel Blanco-Montenegro: Writing – review & editing, Writing – original draft, Visualization, Methodology, Formal analysis, Data curation, Conceptualization. **José Arnoso:** Writing – review & editing, Visualization, Project administration, Investigation, Funding acquisition, Formal analysis, Conceptualization. **Nieves Sánchez:** Writing – review & editing, Investigation, Data curation, Conceptualization. **Fuensanta G. Montesinos:** Writing – review & editing, Project administration, Investigation, Funding acquisition, Conceptualization. **David Gómez-Ortiz:** Writing – review & editing, Visualization, Formal analysis. **Iacopo Nicolosi:** Validation, Methodology, Formal analysis. **Emilio Vélez:** Investigation, Data curation. **Maite Benavent:** Investigation, Formal analysis.

Declaration of competing interest

The authors declare that they have no known competing financial interests or personal relationships that could have appeared to influence the work reported in this paper.

Data availability

Data will be made available on request.

Acknowledgements

This research was financially supported by the projects PID2019-104726GB-I00 of the Spanish Research Agency and CSIC-LAPALMA-07 of the Spanish Ministry of Science and Innovation. Funding for research groups of the Universidad Complutense de Madrid (Financiación Grupos 2021; UCM 2022-GRFN14/22) also supported this work. We wish to thank the Cabildo Insular de La Palma for providing us with facilities to install the magnetic and GNSS stations, and the staff of the Spanish IGN for helping us with the maintenance of the CFU magnetic station. The City Hall of Fuencaliente also supported us with the installation of the SAN magnetic station. We thank the Servicio de Geomagnetismo of the Spanish IGN for providing us with K-indices data from the Güímar geomagnetic observatory. Finally, we acknowledge Associate Editor Yosuke Aoki and two anonymous reviewers for their suggestions and comments which helped us improve the manuscript.

References

Alken, P., Thébault, E., Beggan, C.D., Amit, H., Aubert, J., Baerenzung, J., Bondar, T.N., Brown, W.J., Califf, S., Chambodut, A., Chulliat, A., Cox, G.A., Finlay, C.C., Fournier, A., et al., 2021. International Geomagnetic Reference Field: the thirteenth generation. Earth Planets Space 73, 49. https://doi.org/10.1186/s40623-020-01288-x.

Ancochea, E., Hernán, F., Cendrero, A., Cantagrel, J.M., Fúster, J.M., Ibarrola, E., Coello, J., 1994. Constructive and destructive episodes in the building of a young oceanic island, La Palma, Canary Islands and genesis of the Caldera de Taburiente. J. Volcanol. Geotherm. Res. 60, 243–262.

Benito, M.B., Alvarado, G.E., Marchamalo, M., Rejas, J.G., Murphy, P., Franco, R., Castro, D., Garcia-Lanchares, C., Sanchez, J., 2023. Temporal and spatial evolution of the 2021 eruption in the Tajogaite volcano (Cumbre Vieja rift zone, La Palma, Canary Islands) from geophysical and geodetic parameter analyses. Nat. Hazards 118, 2245–2284. https://doi.org/10.1007/s11069-023-06090-y.

Cabrera-Pérez, I., Soubestre, J., D'Auria, L., Barrancos, J., Martín-Lorenzo, A., van Dorth, D.M., et al., 2023. Geothermal and structural features of La Palma island (Canary Islands) imaged by ambient noise tomography. Sci. Rep. 13 (1), 12892. https://doi.org/10.1038/s41598-023-39910-z.

Camacho, A.G., Fernández, J., González, P.J., Rundle, J.B., Prieto, J.F., Arjona, A., 2009. Structural results for La Palma island using 3-D gravity inversion. J. Geophys. Res. 114, B05411. https://doi.org/10.1029/2008JB005628.

Carracedo, J.C., Badiola, E.R., Guillou, H., de la Nuez, J., Pérez Torrado, F.J., 2001. Geology and volcanology of La Palma and El Hierro, Western Canaries. Estud. Geol. 57, 175–273.

Chouet, B.A., 1996. Long-period volcano seismicity: its source and use in eruption forecasting. Nature 380, 309–316.

Chouet, B.A., 2003. Volcano seismology. Pure Appl. Geophys. 160, 739–788. https://doi.org/10.1007/PL00012556.

Chouet, B.A., Matoza, R.S., 2013. A multi-decadal view of seismic methods for detecting precursors of magma movement and eruption. J. Volcanol. Geotherm. Res. 252, 108–175. https://doi.org/10.1016/j.jvolgeores.2012.11.013.

Currenti, G., Del Negro, C., Johnston, M., Sasai, Y., 2007. Close temporal correspondence between geomagnetic anomalies and earthquakes during the 2002–2003 eruption of Etna volcano. J. Geophys. Res. 112, B09103. https://doi.org/10.1029/2007JB005029.

D'Auria, L., Koulakov, I., Prudencio, J., Cabrera-Pérez, I., Ibáñez, J.M., Barrancos, J., García-Hernández, R., Martínez van Dorth, D., Padilla, G.D., Przeor, M., Ortega, V., Hernández, P., Pérez, N.M., 2022. Rapid magma ascent beneath La Palma revealed by seismic tomography. Sci. Rep. 12, 17654. https://doi.org/10.1038/s41598-022-21818-9.

Davis, P.M., Jackson, D.B., Field, J., Stacey, F.D., 1973. Kilauea volcano, Hawaii: a search for the volcanomagnetic effect. Science 180, 73–74.

Davis, P.M., Pierce, D.R., McPherron, R.L., Dzurisin, D., Murray, T., Johnston, M.J.S., Mueller, R., 1984. A volcanomagnetic observation on Mount St. Helens, Washington. Geophys. Res. Lett. 11, 225–228. https://doi.org/10.1029/GL011i003p00225.

Day, J.M.D., Troll, V.R., Aulinas, M., Deegan, F.M., Geiger, H., Carracedo, J.C., Pinto, G. G., Pérez-Torrado, F.J., 2022. Mantle source characteristics and magmatic processes during the 2021 La Palma eruption. Earth Planet. Sci. Lett. 597, 117793. https://doi.org/10.1016/j.epsl.2022.1177930012-821X.

De Luca, C., Valerio, E., Giudicepietro, F., Macedonio, G., Casu, F., Lanari, R., 2022. Pre- and co-eruptive analysis of the September 2021 eruption at Cumbre Vieja Volcano (La Palma, Canary Islands) through DInSAR measurements and analytical modeling. Geophys. Res. Lett. 49. https://doi.org/10.1029/2021GL097293 e2021GL097293.

Del Fresno, C., Cesca, S., Klügel, A., Domínguez-Cerdeña, I., Díaz-Suárez, E.A., Dahm, T., García-Cañada, L., Meletlidis, S., Milkereit, C., Valenzuela-Malebrán, C., López-Díaz, R., López, C., 2023. Magmatic plumbing and dynamic evolution of the 2021 La Palma eruption. Nat. Commun. 14, 358. https://doi.org/10.1038/s41467-023-35953-y.

Del Negro, C., Ferrucci, F., 1998. Magnetic history of a dyke on Mt Etna. Geophys. J. Int. 133, 451–458.

Del Negro, C., Ferrucci, F., 2000. Volcanomagnetic effects at Vulcano Island (Aeolian archipelago, Italy). Geophys. J. Int. 140, 83–94.

Del Negro, C., Currenti, G., Napoli, R., Vicari, A., 2004. Volcanomagnetic changes accompanying the onset of the 2002–2003 eruption of Mt. Etna (Italy). Earth Planet. Sci. Lett. 229, 1–14. https://doi.org/10.1016/j.epsl.2004.10.033.

Delaney, P.T., 1982. Rapid intrusion of magma into wet rock: Groundwater flow due to pore pressure increases. J. Geophys. Res. 87, 7739–7756.

Di Paolo, F., Ledo, J., Slezak, K., Martínez van Dorth, D., Cabrera-Pérez, I., Pérez, N.M., 2020. La Palma island (Spain) geothermal system revealed by 3D magnetotelluric data inversion. Sci. Rep. 10, 18181. https://doi.org/10.1038/s41598-020-75001-z.

Dzurisin, D., 2003. A comprehensive approach to monitoring volcano deformation as a window on the eruption cycle. Rev. Geophys. 41, 1001. https://doi.org/10.1029/2001RG000107.

Fernández, J., Escayo, J., Zhongbo, H., Camacho, A.G., Samsonov, S.V., Prieto, J.F., Tiampo, K.F., Palano, M., Mallorquí, J.J., Ancochea, E., 2021. Detection of volcanic unrest onset in La Palma, Canary Islands, evolution and implications. Sci. Rep. 11, 2540. https://doi.org/10.1038/s41598-021-82292-3.

Fernández, J., Escayo, J., Camacho, A.G., Palano, M., Prieto, J.F., Zhongbo, H., Samsonov, S.V., Tiampo, K.F., Ancochea, E., 2022. Shallow magmatic intrusion evolution below La Palma before and during the 2021 eruption. Sci. Rep. 12, 20257. https://doi.org/10.1038/s41598-022-23998-w.

Fitterman, D.V., 1979. Theory of electrokinetic-magnetic anomalies in a faulted half-space. J. Geophys. Res. 84, 6031–6040.

Fitterman, D.V., 1981. Correction to "Theory of electrokinetic-magnetic anomalies in a faulted half-space". J. Geophys. Res. 86, 9585–9588.

Goldstein, P., Snoke, A., 2005. SAC Availability for the IRIS Community. Incorporated Institutions for Seismology Data Management Center Electronic Newsletter 7(1), Report #UCRL-JRNL-211140. https://ds.iris.edu/ds/newsletter/vol7/no1/193/sac-availability-for-the-iris-community/.

Goldstein, P., Dodge, D., Firpo, M., Minner, L. 2003 "SAC2000: Signal processing and analysis tools for seismologists and engineers". Invited Contribution to "the IASPEI International Handbook of Earthquake and Engineering Seismology", Edited by WHK Lee, H. Kanamori, P.C. Jennings, and C. Kisslinger, Academic Press, London.

Hernández-Pacheco, A., Valls, M.C., 1982. The historic eruptions of La Palma island (Canaries). Rev. Univ. Azores. Ser. C. Nat. 3, 83–94.
Hurst, A.W., Rickerby, P.C., Scott, B.J., Hashimoto, T., 2004. Magnetic field changes on White Island, New Zealand, and the value of magnetic changes for eruption forecasting. J. Volcanol. Geotherm. Res. 136, 53–70.
IGME, 2021. Delimitación de la lava y evaluación del grado de daños por actividad volcánica. https://info.igme.es/eventos/Erupcion-volcanica-la-palma/copernicus-emsr546.
IGN (Instituto Geográfico Nacional), 1999. Spanish Digital Seismic Network. Dataset/Seismic Network, International Federation of Digital Seismograph Networks. https://doi.org/10.7914/SN/ES.
IGN (Instituto Geográfico Nacional), 2022. Catálogo de terremotos. https://doi.org/10.7419/162.03.2022.
Johnston, M.J.S., 1997. Review of electric and magnetic fields accompanying seismic and volcanic activity. Surv. Geophys. 18, 441–475.
Johnston, M.J.S., Stacey, F.D., 1969. Volcano-magnetic effect observed on Mt Ruapehu, New Zealand. J. Geophys. Res. 93, 6541–6544.
Kanda, W., 2010. A heating process of Kuchi-erabu-jima volcano, Japan, as inferred from geomagnetic field variations and electrical structure. J. Volcanol. Geotherm. Res. 189, 158–171. https://doi.org/10.1016/j.jvolgeores.2009.11.002.
Klügel, A., Hansteen, T.H., Galipp, K., 2005. Magma storage and underplating beneath Cumbre Vieja volcano, la Palma (Canary Islands). Earth Planet. Sci. Lett. 236 (1–2), 211–226.
Konstantinou, K.I., 2024. A Review of the source characteristics and physical mechanisms of very long period (VLP) seismic signals at active volcanoes. Surv. Geophys. 45, 117–149. https://doi.org/10.1007/s10712-023-09800-0.
Lekkas, E., Meletlidis, S., Kyriakopoulos, K., Manousaki, M., Mavroulis, S., Kostaki, I., Michailidis, A., Gogou, M., Mavrouli, M., Castro-Melgar, I., Gatsios, T., Parcharidis, I. 2021. The 2021 Cumbre Vieja volcano eruption in La Palma (Canary Islands). Doi:10.13140/RG.2.2.31086.95040.
Longpré, M.A., Felpeto, A., 2021. Historical volcanism in the Canary Islands; part 1: a review of precursory and eruptive activity, eruption parameter estimates, and implications for hazard assessment. J. Volcanol. Geotherm. Res. 419, 107363. https://doi.org/10.1016/j.jvolgeores.2021.107363.
Montesinos, F.G., Sainz-Maza, S., Gómez-Ortiz, D., Arnoso, J., Blanco-Montenegro, I., Benavent, M., Vélez, E., Sánchez, N., Martín-Crespo, T., 2023. Insights into the magmatic feeding system of the 2021 eruption at Cumbre Vieja (La Palma, Canary Islands) inferred from gravity data modeling. Remote Sens. 15, 1936. https://doi.org/10.3390/rs15071936.
Napoli, R., Currenti, G., Del Negro, C., Greco, F., Scandura, D., 2008. Volcanomagnetic evidence of the magmatic intrusion on 13th May 2008 Etna eruption. Geophys. Res. Lett. 35, L22301. https://doi.org/10.1029/2008GL035350.
Okubo, A., Kanda, W., 2010. Numerical simulation of piezomagnetic changes associated with hydrothermal pressurization. Geophys. J. Int. 181, 1343–1361. https://doi.org/10.1111/j.1365-246X.2010.04580.x.
Ortega-Ramos, V., D'Auria, L., Granja-Bruña, J.L., Cabrera-Pérez, I., Barrancos, J., Padilla, G.D., et al., 2024. Evidence of a low-velocity zone in the upper mantle beneath Cumbre Vieja volcano (Canary Islands) through receiver functions analysis. Geophys. Res. Lett. 51. https://doi.org/10.1029/2023GL105487 e2023GL105487.
Padrón, E., Pérez, N.M., Rodríguez, F., Melián, G.V., Hernández, P.A., Sumino, H., Padilla, G., Barrancos, J., Dionis, S., Notsu, K., Calvo, D., 2015. Dynamics of diffuse carbon dioxide emissions from Cumbre Vieja volcano, La Palma. Canary Islands. Bull. Volcanol. 77, 28. https://doi.org/10.1007/s00445-015-0914-2.
Padrón, E., Pérez, N.M., Hernández, P.A., Sumino, H., Melián, G.V., Alonso, M., Rodríguez, F., Asensio-Ramos, M., D'Auria, L., 2022. Early precursory changes in the 3He/4He ratio prior to the 2021 Tajogaite eruption at Cumbre Vieja volcano, La Palma, Canary Islands. Geophys. Res. Lett. 49. https://doi.org/10.1029/2022GL099992 e2022GL099992.
Parés, J.M., Vernet, E., Calvo-Rathert, M., Soler, V., Bógalo, M.F., Álvaro, A., 2022. Rock magnetism of lapilli and lava flows from Cumbre Vieja Volcano, 2021 eruption (La Palma, Canary Islands): initial reports. Geosciences 12, 271. https://doi.org/10.3390/geosciences12070271.
Parkinson, W.D., 1983. Introduction to Geomagnetism. Scottish Academic Press.
Pozzi, J.P., Le Mouel, J.L., Rossignol, J.C., Zlotnicki, J., 1979. Magnetic observations made on La Soufriere Volcano (Guadeloupe) during the 1976-77 crisis. J. Volcanol. Geotherm. Res. 5, 217–237.
Przeor, M., Castaldo, R., D'Auria, L., Pepe, A., Pepe, S., Sagiya, T., Solaro, G., Tizzani, P., Barrancos Martínez, J., Pérez, N., 2024. Geodetic imaging of magma ascent through a bent and twisted dike during the Tajogaite eruption of 2021 (La Palma, Canary Islands). Sci. Rep. 14, 212. https://doi.org/10.1038/s41598-023-50982-9.
Rodríguez-Pascua, M.Á., Pérez-López, R., Perucha, M.Á., Sánchez, N., López-Gutierrez, J., Mediato, J.F., Sanz-Mangas, D., Lozano, G., Galindo, I., García-Davalillo, J.C., et al., 2024. Active faults, kinematics, and seismotectonic evolution during Tajogaite Eruption 2021 (La Palma, Canary Islands, Spain). Appl. Sci. 14, 2745. https://doi.org/10.3390/app14072745.
Sasai, Y., 1980. Application of the elasticity theory of dislocations to tectonomagnetic modelling. Bull. Earthq. Res. Ins. 55, 387–447.
Sasai, Y., Shimomura, T., Hamano, Y., Utada, H., Yoshino, T., Koyama, S., Ishikawa, I., Yokoyama, Y., Ohno, M., et al., 1990. Volcanomagnetic effect observed during the 1986 eruption of Izu-Oshima Volcano. J. Geomagn. Geoelectr. 42, 291–317.
Sigmundsson, F., Parks, M., Hooper, A., et al., 2022. Deformation and seismicity decline before the 2021 Fagradalsfjall eruption. Nature 609, 523–528. https://doi.org/10.1038/s41586-022-05083-4.
Sparks, R.S.J., 2003. Forecasting volcanic eruptions. Earth Planet. Sci. Lett. 210, 1–15. https://doi.org/10.1016/S0012-821X(03)00124-9.
Stacey, F.D., Barr, K.G., Robson, G.R., 1965. The volcanomagnetic effect. Pure Appl. Geophys. 161, 1433–1452.
Staudigel, H., Schmincke, H.U., 1984. The Pliocene seamount series of La Palma, Canary Islands. J. Geophys. Res. 89, 11195–11215.
Suárez, A.B., Domínguez-Cerdeña, I., Villaseñor, A., Sainz-Maza Aparicio, S., del Fresno, C., García-Cañada, L., 2023. Unveiling the pre-eruptive seismic series of the La Palma 2021 eruption: Insights through a fully automated analysis. J. Volcanol. Geotherm. Res. 444, 107946. https://doi.org/10.1016/j.jvolgeores.2023.107946.
Tanaka, Y., 1993. Eruption mechanism as inferred from geomagnetic changes with special attention to the 1989-90 activity of Aso Volcano. J. Volcanol. Geotherm. Res. 56, 319–338.
Torres-González, P.A., Luengo-Oroz, N., Lamolda, H., D'Alessandro, W., Albert, H., Iribarren, I., Moure-García, D., Soler, V., 2020. Unrest signals after 46 years of quiescence at Cumbre Vieja, La Palma, Canary Islands. J. Volcanol. Geotherm. Res. 392, 106757. https://doi.org/10.1016/j.jvolgeores.2019.106757.
Verhoef, J., Collette, B.J., Dañobeitia, J.J., Roeser, H.A., Roest, W.R., 1991. Magnetic anomalies off West Africa (20–38°N). Mar. Geophys. Res. 13, 81–103.
Yukutake, T., Utada, H., Yoshino, T., Watanabe, H., Hamano, Y., Sasai, Y., Kimoto, E., Otani, K., Shimomura, T., 1990. Changes in the geomagnetic total intensity observed before the eruption of Oshima volcano in 1986. J. Geomag. Geolectr. 42, 277–290.
Zlotnicki, J., Bof, M., 1998. Volcanomagnetic signals associated with the quasi-continuous activity of the andesitic Merapi volcano (Indonesia): 1990-1995. Phys. Earth Planet. Inter. 105, 119–130.
Zlotnicki, J., Le Mouel, J.L., 1988. Volcanomagnetic effects observed on Piton de la Fournaise Volcano (Reunion Island): 1985-1987. J. Geophys. Res. 86, 11899–11909.
Zlotnicki, J., Le Mouel, J.L., Delmond, J.C., Pambrun, C., Delorme, H., 1993. Magnetic variations on Piton de la Fournaise volcano. Volcanomagnetic signals associated with the November 6 and 30, 1987, eruptions. J. Volcanol. Geotherm. Res. 56, 281–296.